TISSUE ENGINEERING: Part A
Volume 17, Numbers 5 and 6, 2011

DOI: 10.1089/ten.tea.2010.0404

Selective Activation of Sphingosine 1-Phosphate Receptors 1 and 3 Promotes Local Microvascular Network Growth

Lauren S. Sefcik, Ph.D.,[1] Caren E. Petrie Aronin, Ph.D.,[2] Anthony O. Awojoodu, B.S.,[3] Soo J. Shin, B.S.,[3] Feilim Mac Gabhann, Ph.D.,[4] Timothy L. MacDonald, Ph.D.,[5] Brian R. Wamhoff, Ph.D.,[6,7] Kevin R. Lynch, Ph.D.,[8] Shayn M. Peirce, Ph.D.,[3] and Edward A. Botchwey, Ph.D.[3,9,10]

Proper spatial and temporal regulation of microvascular remodeling is critical to the formation of functional vascular networks, spanning the various arterial, venous, capillary, and collateral vessel systems. Recently, our group has demonstrated that sustained release of sphingosine 1-phosphate (S1P) from biodegradable polymers promotes microvascular network growth and arteriolar expansion. In this study, we employed S1P receptor-specific compounds to activate and antagonize different combinations of S1P receptors to elucidate those receptors most critical for promotion of pharmacologically induced microvascular network growth. We show that $S1P_1$ and $S1P_3$ receptors act synergistically to enhance functional network formation via increased functional length density, arteriolar diameter expansion, and increased vascular branching in the dorsal skinfold window chamber model. FTY720, a potent activator of $S1P_1$ and $S1P_3$, promoted a 107% and 153% increase in length density 3 and 7 days after implantation, respectively. It also increased arteriolar diameters by 60% and 85% 3 and 7 days after implantation. FTY720-stimulated branching in venules significantly more than unloaded poly(D, L-lactic-co-glycolic acid). When implanted on the mouse spinotrapezius muscle, FTY720 stimulated an arteriogenic response characterized by increased tortuosity and collateralization of branching microvascular networks. Our results demonstrate the effectiveness of $S1P_1$ and $S1P_3$ receptor-selective agonists (such as FTY720) in promoting microvascular growth for tissue engineering applications.

Introduction

Effective strategies to control microvascular network growth are critical to improving the treatment of ischemic tissue diseases and to enhancing the regenerative capacity of implant materials. However, there is emerging recognition that capillary network expansion via angiogenesis often does not compensate for inadequate arteriolar blood flow to ischemic tissues, and that the growth of microvascular networks must be accompanied by vascular maturation and remodeling, whereby pericytes and vascular smooth muscle cells (SMCs) are recruited to these nascent vessels.[1] This latter process may also have been referred to as capillary arterialization,[2] arteriolar genesis,[3] or more broadly, arteriogenesis, the results of which being the new growth and structural enlargement of functional arterioles.[4,5] Thus, the ability to increase the number and diameter of resistance microvessels that are critical to improving blood flow must rely on a multitude of biological signals, including molecular regulators of arteriogenesis.

Sphingosine 1-phosphate (S1P) is a bioactive sphingolipid that serves as a ligand for five known G protein-coupled receptors. It has been shown to stimulate endothelial cell (EC) proliferation and migration[6,7] and to recruit pericytes and SMCs to immature vessels so that they may proliferate, migrate, and differentiate to a more contractile phenotype.[8–11] Three of S1P's five receptors are expressed at high levels on ECs and SMCs: $S1P_1$, $S1P_2$, and $S1P_3$ (Fig. 1). Importantly, these three receptors are coupled to different and opposing signaling cascades. $S1P_1$ is coupled specifically to G_i proteins,

[1]Department of Chemical and Biomolecular Engineering, Lafayette College, Easton, Pennsylvania.
[2]National Institute of Allergy and Infectious Diseases, National Institutes of Health, Bethesda, Maryland.
[3]Department of Biomedical Engineering, University of Virginia, Charlottesville, Virginia.
[4]Institute for Computational Medicine and Department of Biomedical Engineering, Johns Hopkins University, Baltimore, Maryland.
Departments of [5]Chemistry and [6]Cardiovascular Medicine, University of Virginia, Charlottesville, Virginia.
[7]The Robert M. Berne Cardiovascular Research Center, Charlottesville, Virginia.
Departments of [8]Pharmacology and [9]Orthopaedic Surgery, University of Virginia, Charlottesville, Virginia.
[10]Center for Immunity, Inflammation and Regenerative Medicine, University of Virginia, Charlottesville, Virginia.

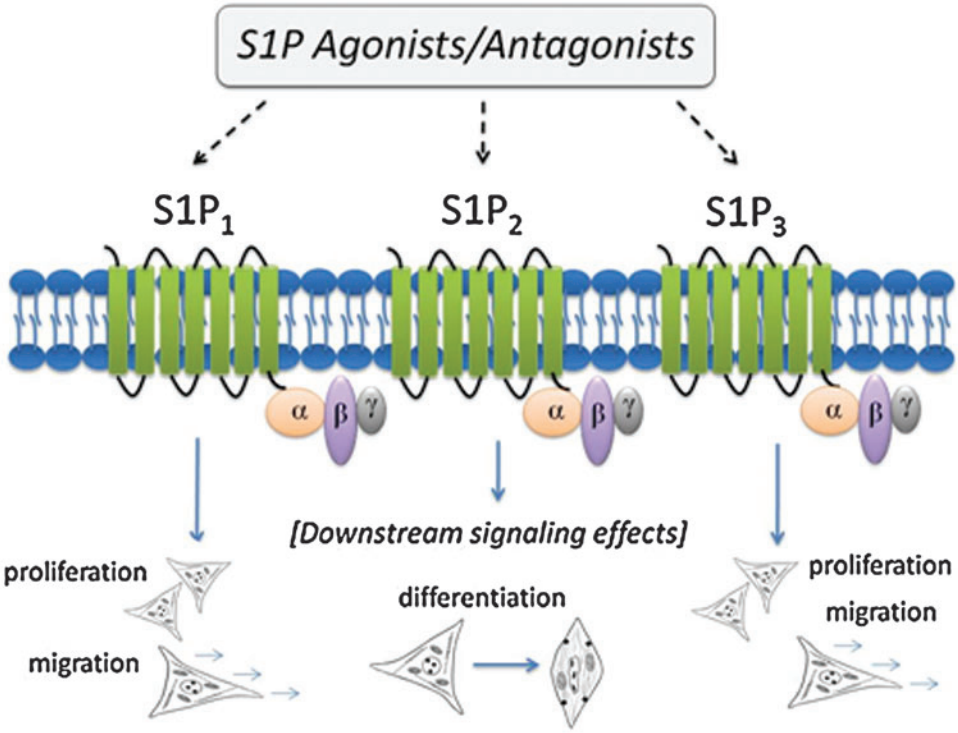

FIG. 1. Sphingosine 1-phosphate (S1P) signals through a family of G protein-coupled receptors: $S1P_1$–$S1P_5$. Receptors $S1P_1$, $S1P_2$, and $S1P_3$ are found on vascular endothelial cells and smooth muscle cells. Receptor-specific activation using a library of agonists and antagonists (Table 1) can be used to modulate downstream cell fate processes. Smooth muscle cells (depicted above in cartoons) undergo phenotypic modulation from a synthetic (proliferative) state to a contractile (differentiated) state dependent upon S1P receptor activation. Color images available online at www.liebertonline.com/ten.

Table 1. Vascular-Related Effects of Sphingosine 1-Phosphate Receptor Agonists and Antagonists

Compound	*Agonist activity*	*Antagonist activity*	*Vascular-related effects*
S1P	$S1P_1$ $S1P_2$ $S1P_3$ $S1P_4$[a] $S1P_5$[a]		Increases EC, SMC proliferation, and migration via $S1P_1$ (Kluk and Hla,[10] Lockman *et al.*[11]) Inhibits SMC migration via $S1P_2$ (Saba and Hla[39]) Stimulates SMC differentiation to contractile phenotype via $S1P_2$ (Lockman *et al.*[11])
FTY720	$S1P_1$ $S1P_3$ $S1P_4$[a] $S1P_5$[a]		Inhibits VEGF-induced vascular permeability, mediates EC adherens junction formation, and increases EC survival (Sanchez *et al.*[25]) Enhances EC migration (Butler *et al.*[40]) Decreases EC, SMC proliferation at high doses (>1 μM) (Schmid *et al.*[27])
VPC01091	$S1P_1$ $S1P_4$[a] $S1P_5$[a]	$S1P_3$	Increases neointimal hyperplasia (SMC proliferation) after acute balloon injury (Wamhoff *et al.*[24])
JTE013		$S1P_2$	Increases EC, SMC migration (Osada *et al.*[41]) Improves diabetic wound healing (Kawanabe *et al.*[42]) Increases SMC proliferation, suppresses S1P-induced SMC differentiation (Wamhoff *et al.*[24]) Enhances EC tube formation (Inoki *et al.*[43])
VPC44116		$S1P_1$ $S1P_3$	Attenuates neointimal hyperplasia (SMC proliferation) after acute balloon injury (Wamhoff *et al.*[24])

[a]$S1P_4$ and $S1P_5$ are not found on ECs and SMCs.
EC, endothelial cell; SMC, smooth muscle cell; S1P, sphingosine 1-phosphate; VEGF, vascular endothelial growth factor.

and both $S1P_2$ and $S1P_3$ are coupled to G_i, G_q, and G_{12} proteins.[12] The activation of these different G proteins, including G_i for proliferation, G_{12} for cytoskeletal remodeling, and G_q for cellular effects, is elicited by S1P binding to its receptors on vascular cells.[13,14] To this end, a general paradigm has emerged that $S1P_1$/$S1P_3$ signaling promotes SMC proliferation and migration, whereas $S1P_2$ has opposing actions. Activating and/or antagonizing specific combinations of these three S1P receptors on ECs and SMCs may be an effective strategy for promoting arteriogenesis in ischemic tissues by inducing SMC proliferation and the growth of functional arteriolar microvessels (Table 1).

Effective *in vivo* models to monitor both temporal and spatial changes in microvascular growth and remodeling are critical in assessing the affects of pharmacological inducers of arteriogenesis. The dorsal skinfold window chamber model

has been established as an efficient model to track the temporal and spatial changes of vessels in the subcutaneous microcirculation of mice.[15,16] This model allows for intravital monitoring and quantitative assessment of changes occurring in the microvascular network for several weeks. Further, the architecture of the window chamber is conducive to implantation of a variety of different drug delivery systems and the stimulated tissue can easily be excised and examined with precise spatial reference to the implant using a variety of techniques (e.g., histology and immunohistochemistry).[17] To study whole-network level microvascular remodeling in intact tissues, the spinotrapezius model has proven very useful in studying environmental factors in skeletal muscle while retaining spatial resolution.[18,19] The ability to expose the muscle to bolus injections or drug-releasing implants, to alter its local microenvironment, and to observe the changes in arterioles *in situ* makes this model very useful for measuring arteriogenesis. The muscle can also be excised for more specific whole-mount immunohistochemical analysis, preserving the spatial resolution of the vascular network. In this work, we capitalize on the spatio-temporal advantages of both the dorsal skinfold window chamber model and the spinotrapezius model in C57Bl/6 mice to interrogate the roles of specific S1P receptors in the microvascular environment.

Considering the establishment of S1P as a key signaling molecule in vascular ECs and SMCs during both development and adult wound healing, and its demonstrated effectiveness in *in vitro* models of angiogenesis, there is surprisingly little known regarding its therapeutic potential for stimulating whole-network level microvascular remodeling *in vivo*. To this end, analysis of S1P receptor-specific signaling in the microvasculature is necessary if therapeutic strategies aimed at the induction of neovascularization are to be realized. In this work, we systematically evaluate the physiological responses of microvascular networks to varying patterns of S1P receptor targeting and activation at the tissue level. Activating and antagonizing different combinations of S1P receptors allows us to elucidate those receptors most critical for promotion of pharmacologically induced arteriogenesis. Our results demonstrate that S1P receptor-selective pharmacologic agents can be utilized to locally induce neovascularization and the formation of a mature vasculature, which has long-ranging implications in all areas of tissue repair and remodeling.

Materials and Methods

Materials

Poly(D, L-lactic-co-glycolic acid) (PLAGA) in a 50:50 formulation (71 kDa) was purchased from Lakeshore Biomaterials. S1P (379.5 Da), FTY720 (307.5 Da), and JTE013 (408.3 Da) were purchased from Cayman Chemical. The prodrug compounds VPC01091 (303.3 Da) and VPC44116 (451.3 Da) were synthesized in the laboratories of Drs. Macdonald and Lynch at the University of Virginia.

Fabrication of PLAGA thin films

PLAGA thin polymeric films (1 mm diameter and 0.5 mm height) were cast unloaded to be used as controls or loaded

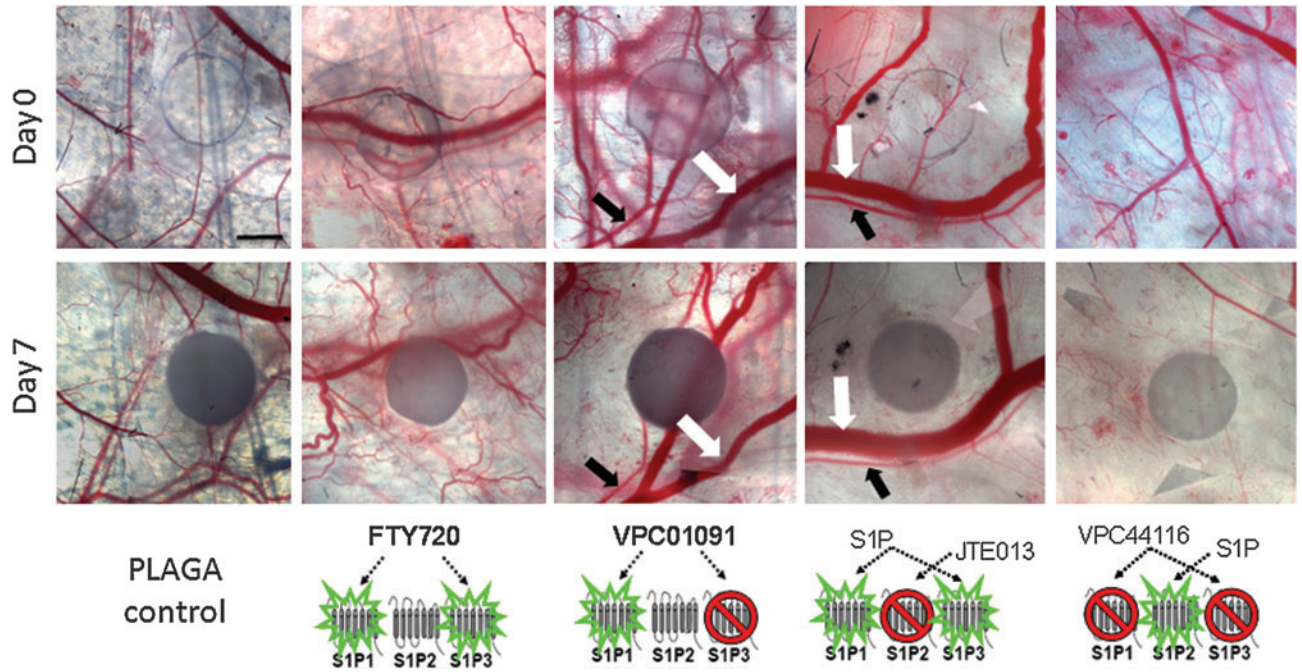

FIG. 2. $S1P_1$, $S1P_3$ activation with FTY720 enhances microvascular remodeling in window chamber. Intravital microscopy images of poly(D, L-lactic-co-glycolic acid) (PLAGA) films loaded with FTY720, VPC01091, S1P+JTE013, or S1P+VPC44116 in the dorsal skinfold window chamber at 0 and 7 days postimplantation of films. Substantial increases in new vascular growth are seen in response to FTY720. VPC01091, JTE013, and VPC44116 decrease functional length density over 7 days. Examples of venules are denoted by white arrows, and arterioles by black arrows. Blood column width is the diameter of the blood vessels as seen in intravital images and used to quantify changes in vessel diameter. Scale bar = 500 μm. Color images available online at www.liebertonline.com/ten.

with (1) 1:400 (wt./wt., drug/PLAGA) S1P:PLAGA; (2) 1:200 VPC01091:PLAGA; (3) 1:200 FTY720:PLAGA; (4) 1:2:400 S1P:JTE013:PLAGA; or (5) 1:2:400 S1P:VPC44116:PLAGA. Briefly, the desired drug was solubilized in methylene chloride in a borosilicate scintillation vial using alternating cycles of heating (65°C water bath) and vortexing until completely dissolved. For films containing two drugs (S1P+JTE013 or S1P+VPC44116), each drug was solubilized separately and then combined into one vial containing PLAGA. Dissolved drug:polymer solutions were solvent-cast in a Teflon mold, lyophilized for 24 h to extract any remaining solvent (Labconco Corp.), and extracted for implantation using a 1 mm biopsy punch (Acuderm, Inc.).

Dorsal skinfold window chamber surgical procedure and image acquisition

Animal experiments were performed using sterile techniques in accordance with an approved protocol from the University of Virginia Animal Care and Use Committee. Male C57Bl/6 mice (Harlan), age-matched (6–8 weeks) and weighing between 18 and 25 g, were surgically fitted with dorsal skinfold window chambers (APJ Trading Company, Inc.). After a waiting period of 7 days, control or drug-loaded films were implanted into the window chamber (referred to as day 0) and imaged on days 3 and 7 post-implantation. For details, see Sefcik *et al.*[15] and Wieghaus and coworkers.[15]

Quantitative microvascular metrics

Intravital microscopy montages of entire vascular windows at days 0, 3, and 7 were analyzed using a combination of Adobe Photoshop CS and ImageJ (http://rsb.info.nih.gov/ij/) software. Blood vessels were analyzed within a circular region of interest (ROI) centered around the 1-mm-diameter polymer film and extending 2 mm from the outer edge of the film (area of ROI is a circle of diameter 5 mm, or 19.6 mm^2, see Fig. 3 in Wieghaus and coworkers[15]). For microvascular length density measurements, vessels located within the ROI were traced using Photoshop and skeletonized using ImageJ. These binary images were then analyzed by counting the total number of black (vs. white) pixels, representing the total length of all traced vessels. Pixels were converted to mm using a micrometer and divided by the total area of the ROI to yield length density. To assess changes in lumenal diameter, arteriole–venule pairs were identified within the ROIs. In intravital images, vessels are observed by blood column width, which is defined as the diameter of a perfused blood vessel as viewed under intravital microscopy in two dimensions. Therefore, arterioles and venules identified as a pair were labeled on day 0 on the basis of size only—venule diameters

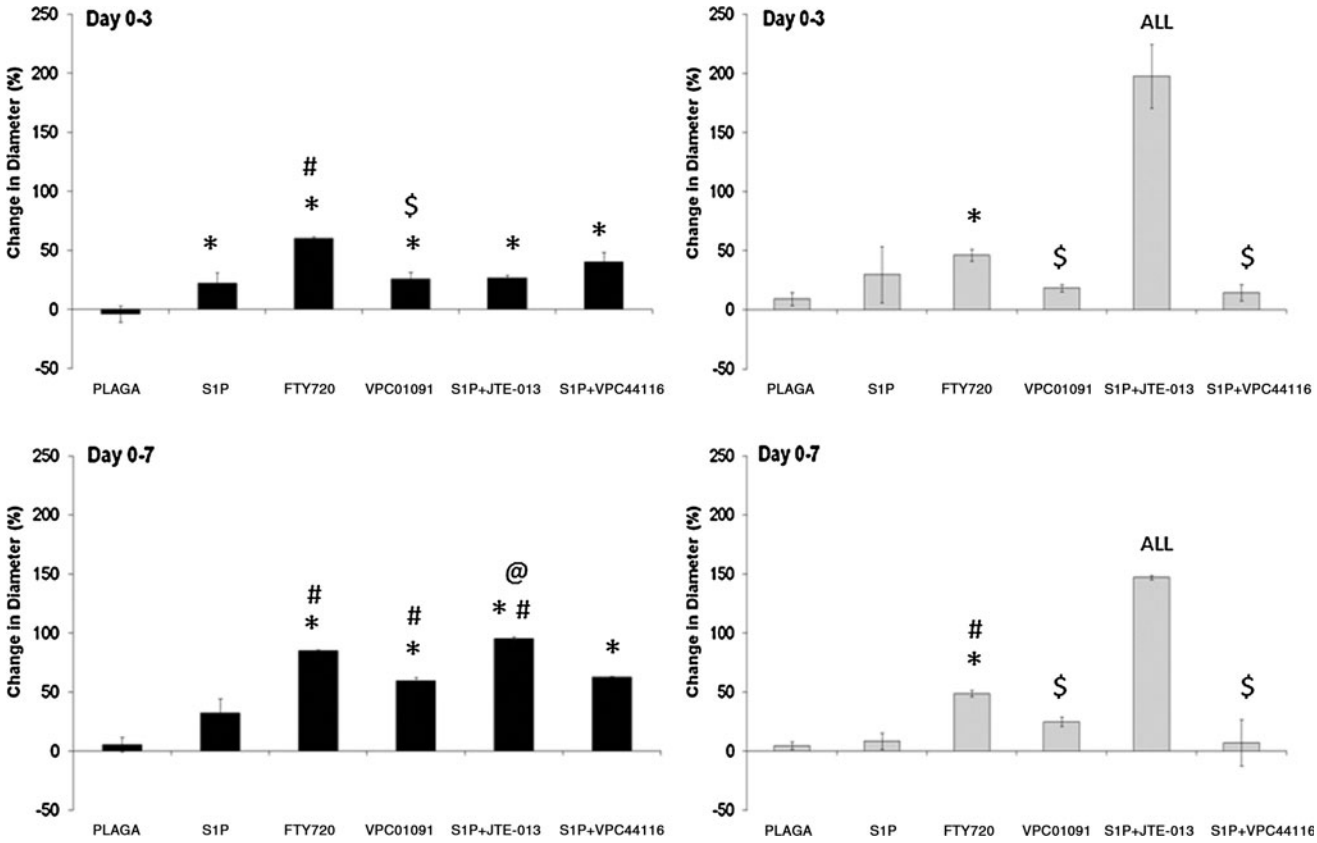

FIG. 3. Effect of S1P receptor-selective activation on arteriolar (left) and venular (right) diameters after 3 (top) and 7 (bottom) days of treatment with 1 mm PLAGA control films or PLAGA films loaded with S1P agonists and antagonists. Selective activation of $S1P_1$ and $S1P_3$ (with FTY720 or S1P+JTE013) significantly increased both arteriolar and venular diameters compared to S1P itself. Bars from left to right: PLAGA, S1P, FTY720, VPC01091, S1P+JTE013, and S1P+VPC44116. $p < 0.05$, relative to *PLAGA; #S1P; @VPC01091; $FTY720; ALL, all venule groups.

were larger than arteriolar diameters on day 0 (see Fig. 2 for arrows distinguishing arterioles and venules on day 0). Identical vessel segments were labeled on days 0, 3, and 7 images at the bisection of each vessel segment in between branch points. Internal diameters based on blood column widths were measured using ImageJ. The number of branch points was quantified by marking a point of bifurcation on a blood vessel at days 0, 3, and 7. This vessel branch was then followed and bifurcations were marked. These new branches were also tracked and marked at points of bifurcations; thus, branch points three degrees of freedom away from the parent vessel were quantified. The number of branch points at days 3 and 7 were normalized to the number present at day 0. For length density, diameter, and branching metrics, the limit of resolution of vessels that can be observed is 10 μm; thus, capillaries (<10 μm) are not included in these analyses.

Tissue harvest and histological analysis of window chamber tissues

After the final imaging of the dorsal skinfold window chamber on day 7, mice were euthanized for tissue harvest with an overdose of Nembutal administered intraperitoneally. Immediately, the chest cavity was opened and the vasculature was perfused with 10 mL of 1×Tris-buffered saline plus 0.1 mM $CaCl_2$ and 2% heparin via the right ventricle, followed by 10 mL of 1×Tris-buffered saline plus 0.1 mM $CaCl_2$ and 10 mL 4% paraformaldehyde for vessel fixation. During this time, 4% paraformaldehyde was dripped onto the exposed vascular region of the window chamber. After perfusion and fixation, the window chamber tissue was excised using surgical microscissors. Tissues were embedded in paraffin, sectioned into 5-μm-thick slices, and mounted onto glass slides by the University of Virginia Histology Core Facility. Paraffin sections were de-paraffinized and rehydrated using xylenes and a graded series of ethanol washes.[15] Sections were washed in phosphate-buffered saline containing 0.1% saponin and 2% bovine serum albumin (PBS/saponin/BSA) 3×10 min each. Each tissue section was immunolabeled for smooth muscle α-actin (SMA) using CY3-conjugated monoclonal anti-SMA (Sigma) diluted 1:500 in PBS/saponin/BSA and then mounted using a 50:50 solution of PBS and glycerol. Stained sections were imaged using a Nikon TE 2000-E2 confocal microscope equipped with a Melles Griot Argon Ion Laser System and Nikon D-Eclipse C1 accessories. Representative images were acquired using a 60x/1.45 NA Nikon oil immersion objective and Nikon EZ-C1 software. The area of histological tissue sections was calculated by first outlining and then measuring the entire sections using ImageJ. The number of microvessels with obvious lumens staining positive for SMA were counted under 10×magnification and then divided by the total sectional area. The limit of resolution for SMA+, an SMC marker, microvessels with an obvious lumen at 10×was ~6 μm, which could include capillaries.

Spinotrapezius surgical procedure

Male C57Bl/6 mice (Harlan), age matched and weighing between 18 and 25 g, were used for spinotrapezius surgeries. Mice were anesthetized via intraperitoneal injection of ketamine/xylazine/atropine (80/8/0.08 mg/kg), shaved, and depilated. Surgical procedures detailed by Bailey *et al.*[18] and Mac Gabhann and Peirce[19] were modified to accompany PLAGA film implantation. A horse-shoe-shaped incision (~3–5 mm) was made through the dorsal skin, ~5 mm caudal to the bony prominence of the shoulder blade. Under a dissecting microscope, a characteristic knot structure of an artery–vein pair located at the caudal-lateral edge of the muscle was identified. The artery was traced up to the cranial end of the muscle, passing a classic loop structure, and eventually leaving the muscle and traversing a fat pad. The classic loop structure was used as a guide to mark the location to insert the polymer film. Above this location, the overlying fascia was blunt dissected to create a pocket a few millimeters in diameter. The 1 mm polymer film was then carefully placed into this pocket and the fascial layer was pulled back over top of the polymer. In this manner, the polymer stayed in place on top of the muscle. All implants were inserted into the right spinotrapezius muscle, with the left muscle serving as an internal control. The dorsal skin incision was then closed with 8-0 Ethilon sutures (Ethicon, Inc.), and the animal was allowed to recover on a heating pad. Warmed Ringer's solution (37°C) with adenosine (1 mM), a potent vasodilator, was superfused onto the tissue throughout the surgery to aid in the observation of vessel architecture. Intravital images were taken during the surgical procedure using an Olympus Microfire (Olympus) color digital camera.

Harvest and staining of whole-mount spinotrapezius tissues

On day 7 after polymer implantation, mice were euthanized and perfusion-fixed using methods described above. Both the left (untreated control) and right (treated) spinotrapezius muscles were stripped of the overlying fascia and excised. The polymer films were removed before staining to better observe the vasculature underneath the polymer. Tissues were washed in PBS/saponin/BSA 3×10 min each and then stained for SMA (IA4-Cy3; Sigma, 1 mg/mL) at room temperature for 1 h and then overnight at 4°C. The tissues were then washed with PBS, mounted on glass slides using 50:50 PBS/glycerol, and imaged using confocal microscopy.

Statistical analyses

All statistical analyses were performed using Minitab 15 statistical software (Minitab, Inc.). Results are presented as mean ± standard error of the mean. Comparisons were made using a one-way analysis of variance, followed by Tukey's test for pairwise comparisons. Diameter analysis was performed using a General Linear Model analysis of variance with an unbalanced nested design, followed by Tukey's test for pairwise comparisons. Significance was asserted at $p < 0.05$. Power calculations were performed with $\alpha = 0.05$ and power = 0.80 to determine statistically significant sample size.

Results

$S1P_1$, $S1P_3$ synergism enhances microvascular growth and remodeling

We hypothesized that by selectively activating the two receptors known to stimulate EC and SMC proliferation and migration ($S1P_1$, $S1P_3$), both new vascular growth and vessel maturation would be significantly enhanced over time. To test this hypothesis, we delivered FTY720 ($S1P_1$, $S1P_3$ agonist)

in a controlled manner from 1 mm thin films of PLAGA and assessed its ability to locally stimulate microvascular growth after a period of 3 and 7 days in the window chamber. Previously, we reported on an unsteady state mass transport model to approximate the release kinetics of S1P from the polymer into the tissue space ([S1P] = 264 nM after 7 days at a distance of 1 mm away from the film).[15] Data from our lab using radiolabeled ^{33}P-S1P validated the model with S1P concentrations of ~500 nM in the tissue after 7 days within a distance of 1 mm from the film. Qualitative intravital microscopy images (Fig. 2) of FTY720-stimulated tissues show substantial increases in new microvessel growth, which was confirmed quantitatively by diameter and length density metrics, suggesting a release of FTY720 from PLAGA in a concentration that stimulates cell proliferation and migration.

Treatment with FTY720 significantly increased the lumenal diameters of both arterioles and venules after 3 and 7 days compared to the unloaded PLAGA control or S1P itself (Fig. 3). Diameter measurements were binned by initial diameter (diameter at day 0) as <30 μm for arterioles or <50 μm for venules). A closer examination into the size range of arterioles undergoing lumenal expansion in response to FTY720 revealed that arterioles with the smallest range of initial diameters on day 0 (<30 μm) underwent the most significant increase in diameter expansion compared to other size ranges. Additionally, FTY720 treatment significantly increased the diameter of the largest size arterioles (those binned >50 μm at day 0) compared to PLAGA and S1P-treated tissues after 7 days, making it an attractive candidate for increasing local blood flow to ischemic tissues by enlarging the size of pre-existing vessels (data not shown).

Venular remodeling was similar to the trends observed in arterioles in response to FTY720 treatment. After 3 days of exposure to FTY720-loaded films, venules significantly increased in blood column width, relative to unloaded controls (Fig. 3). After 7 days of treatment, FTY720 elicited statistically significant increases in venular diameter expansion compared to both control and S1P-treated tissues. As was the case with arterioles, venules in the smallest range of initial diameters (<50 μm) underwent significant increases in diameter expansion compared to sub-50 μm venules in control or S1P-treated tissues after 3 and 7 days (data not shown).

Microvascular length density was also significantly increased after 3 and 7 days, relative to PLAGA- and S1P-treated tissues (Fig. 4). Increased functional length density signifies an increase in the total length of blood vessels with blood column widths >10 μm (in diameter). Thus, an increase in length density may occur by an increase in angiogenesis, by the sprouting of vessels from pre-existing vessels, or by a vascular maturation mechanism whereby existing capillaries (<10 μm) recruit perivascular support cells and increase in size to point of visibility (>10 μm) in the window chamber. To examine the angiogenic effect of FTY720, the number of branch points within the vascular networks was quantified. Results demonstrate a significant increase in the number of branch points in venules after both 3 and 7 days of treatment with FTY720 compared to PLAGA control (Fig. 5). Because angiogenic sprouts most often form from venules, it is not surprising that there is no significant difference in arteriolar branching between FTY720 and PLAGA.

To assess if the increase in length density from FTY720 treatment was also a function of enhanced vascular maturation (increased SMC coverage), dorsal skinfold window chamber tissue was harvested after 7 days and histologically sectioned and stained for SMA, a marker for SMCs. FTY720-treated tissues showed a significant increase in the numbers of SMA positively stained microvessels (SMA+) compared to untreated controls (Fig. 6). However, there was no statistical difference in SMA+microvessels per area between S1P- and FTY720-treated tissues.

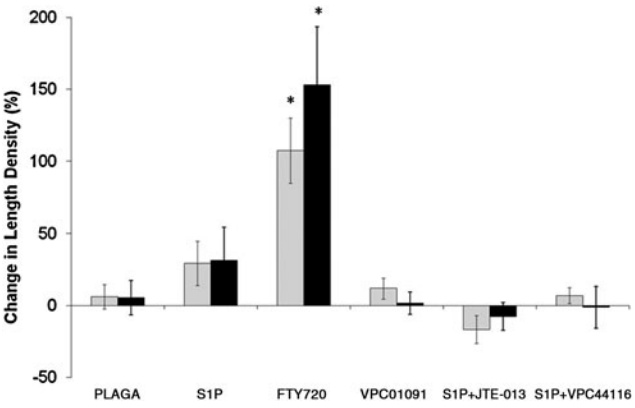

FIG. 4. Effect of S1P receptor signaling modulation on functional length density after 3 (gray bars) and 7 (black bars) days of treatment with 1 mm PLAGA control films or PLAGA films loaded with S1P agonists and antagonists. $S1P_1$, $S1P_3$-selective agonism with FTY720 significantly increased functional microvascular length density. Bars from left to right: PLAGA, S1P, FTY720, VPC01091, S1P+JTE013, and S1P+VPC44116. *$p < 0.05$, significant to all other groups within respective time period (days 0–3, days 0–7).

Selective antagonism of $S1P_3$ diminishes microvascular growth and remodeling mediated by $S1P_1$, $S1P_3$

Local delivery of FTY720 to window chamber tissue significantly increased neovascularization and vessel maintenance over 7 days *in vivo* compared to S1P itself, suggesting that local activation of $S1P_1$ and $S1P_3$ acts synergistically to enhance EC and SMC proliferation and migration. We next evaluated the individual contributions of both of these receptors by delivering VPC01091, a $S1P_1$ agonist and $S1P_3$ antagonist.[20] Local sustained release of VPC01091 significantly decreased arteriolar diameters after 3 days in comparison to FTY720-treated tissues (Fig. 3). Although this trend persisted after 7 days, comparison between VPC01091 and FTY720 was no longer significant. Release of VPC01091 also significantly decreased the lumenal diameters of venules, compared to FTY720, after both 3 and 7 days of stimulation (Fig. 3). There was no statistical difference in venular expansion between PLAGA-, S1P-, or VPC01091-treated tissues.

There was a clearly observable decrease in vascular density over time with VPC01091 treatment compared to PLAGA and FTY720 groups (Fig. 2). Antagonism of $S1P_3$ via delivery of VPC01091 resulted in a significant decrease in vascular length density (Fig. 4) at both days 3 and 7 compared to FTY720 treatment. However, there was no statistical difference between PLAGA-, S1P-, and VPC01091-treated tissues.

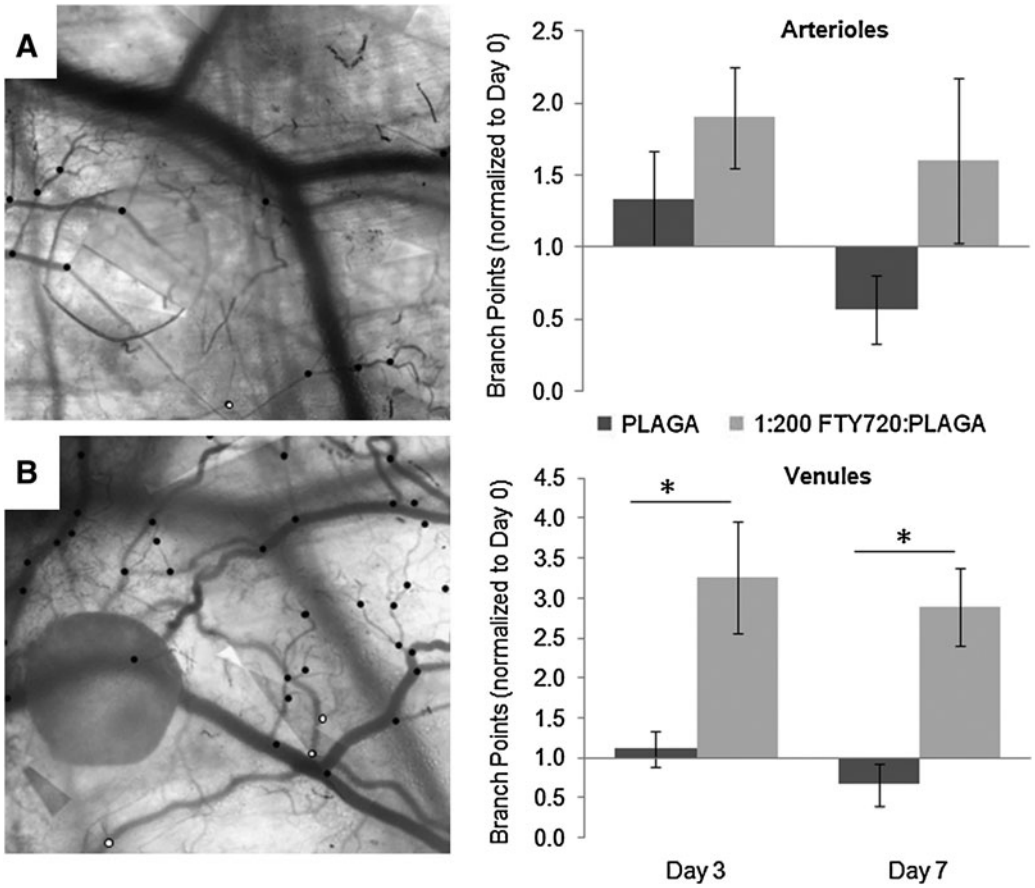

FIG. 5. FTY720 stimulates increased vessel branching in venules, a metric of angiogenesis. The number of branch points on arterioles and venules were quantified after 3 and 7 days of treatment with FTY720. Data were normalized to the number of branch points at day 0 (before drug stimulation). Representative images of increased branching due to FTY720 stimulations are shown in **(A)** (day 0) and **(B)** (day 7). Dots denote location of branch points (white, arterioles; black, venules). $*p < 0.05$, two-sample *t*-test.

VPC01091 treatment also significantly decreased the numbers of SMA+vessels per area compared to FTY720 treatment (Fig. 6). Treatment with VPC01091 also appeared to result in fewer SMA+vessels per area compared to S1P itself, although not statistically significant. Taken together, these results imply that $S1P_1/S1P_3$ receptor synergism by FTY720 elicits a more robust response than $S1P_1$ signaling alone (by VPC01091) in terms of vessel remodeling and overall network maintenance.

Selective inhibition of $S1P_2$ stimulates microvascular lumenal diameter expansion

FTY720 was shown to elicit robust microvascular remodeling responses. To support the hypothesis that $S1P_1$ and $S1P_3$ act synergistically to enhance vascular density and increase diameters, we codelivered S1P with $S1P_2$ antagonist JTE013 and quantified the same remodeling metrics in the dorsal skinfold window chamber. If synergistic activation of $S1P_1$ and $S1P_3$ are required for maximal increases in length density and diameter expansion and $S1P_2$ is not involved, it is hypothesized that S1P+JTE013 should mimic the actions of FTY720 and stimulate robust microvascular remodeling responses. Polymer films containing S1P and JTE013 were implanted into the window chamber and vascular metrics were assessed after 3 and 7 days. Representative intravital images reveal a decrease in vascular density, but an apparent increase in venular blood column width (Fig. 2). Quantitative evaluation of the vascular networks treated with S1P+JTE013 in fact revealed a significant increase in venular expansion after both 3 and 7 days, compared to all drug groups, including FTY720. This result could potentially be attributed to the difference in $S1P_2$ signaling between codelivery of S1P and JTE013 and delivery of FYT720; JTE013 is an antagonist at $S1P_2$, whereas $S1P_2$ remains available for signaling by endogenous S1P during FTY720 treatment. Arteriolar diameters also expanded after both 3 and 7 days relative to PLAGA control, but with no statistical difference to FTY720 treatment (Fig. 3).

Contradictory to lumenal expansion data, S1P+JTE013 significantly decreased total functional length density of microvascular networks over time relative to FTY720 (Fig. 4). After 7 days, there was no statistical difference in length density between control and S1P+JTE013-treated tissues. Taken together, these data examining the potential synergism of $S1P_1$ and $S1P_3$ receptors via two different mechanisms (S1P+JTE013 vs. FTY720) highlight the complexity of both microvascular remodeling and the role that S1P receptor-specific signaling plays in this process.

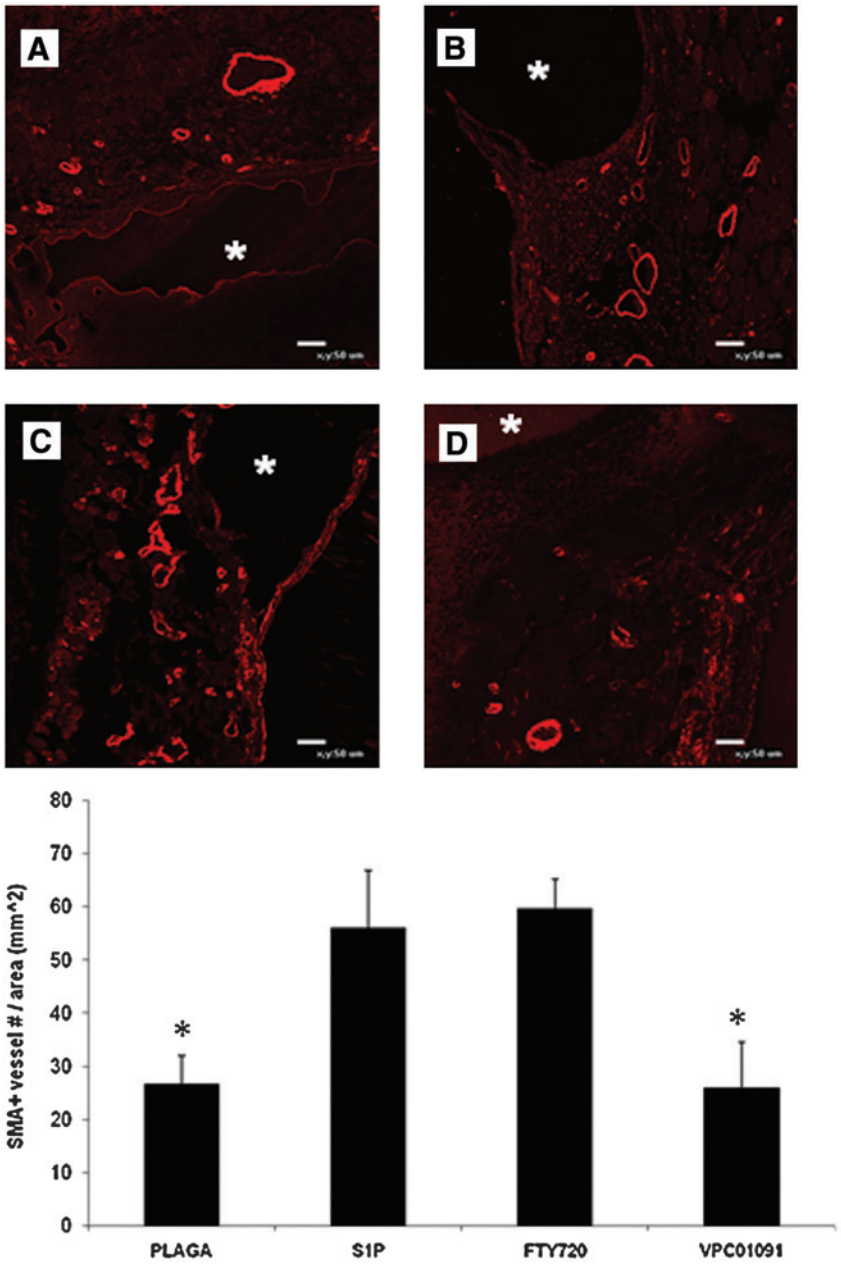

FIG. 6. S1P receptor-selective activation increases the number of smooth muscle α-actin (SMA)+microvessels. Representative images of SMA-stained sections of dorsal skinfold window chamber tissue after 7 days of treatment with unloaded **(A)** PLAGA, **(B)** S1P, **(C)** FTY720, or **(D)** VPC01091. Locations of implanted films are denoted with an asterisk. SMA+vessels per tissue section was quantified. $^*p < 0.05$, significant to FTY720. Color images available online at www.liebertonline.com/ten.

Selective antagonism of S1P1 and S1P3 inhibits microvascular remodeling

Since $S1P_1$ and $S1P_3$ receptors appear to act synergistically to enhance microvascular remodeling in the dorsal skinfold window chamber, we hypothesized that selectively inhibiting $S1P_1$ and $S1P_3$ signaling would thereby prevent microvascular growth and remodeling. VPC44116, a selective $S1P_1$ and $S1P_3$ antagonist, was coencapsulated with S1P and delivered to the window chamber. Microvascular metrics were assessed after 3 and 7 days of stimulation. As expected, the increase in venular diameter in response to FTY720 and S1P+JTE013 treatment after 3 and 7 days was reduced (Fig. 3). Interestingly, this did not hold true for arterioles, as there was not a significant reduction in arteriolar diameter after 7 days compared to FTY720 or S1P+JTE013 treatment. Figure 2 shows representative intravital images of the stark decrease in vascular density observed by S1P+VPC44116 treatment. Upon quantitative assessment, S1P+VPC44116 significantly reduced the increase in functional length density resulting from FTY720 treatment. There was no statistical difference in length density between PLAGA, S1P, VPC01091, or, most surprisingly, S1P+JTE013 treatment.

Effects of local sustained release of S1P receptor-targeted compounds in the spinotrapezius model

Although the dorsal skinfold window chamber model is an excellent tool to observe and quantify precise changes in growth and remodeling of the same microvascular

networks over time, the remodeling responses of the subcutaneous microvasculature may differ from the response in skeletal muscle, a tissue that is classically used to assess arteriogenesis and remodeling in response to ischemia.[21,22] The spinotrapezius muscles are a pair of skeletal muscles located on the dorsum adjacent to either side of the spine and running between the fourth thoracic and third lumbar vertebrae in mice. The mouse spinotrapezius is well perfused with highly developed collateral vessels and arcade arteriole loops in C57Bl/6 mice, and is only 60–200 μm thick, thus allowing *en face* observation of the muscle tissue and microvascular networks.[18,19] To investigate if the effects of S1P-targeted compounds on microvascular remodeling in the subcutaneous tissue (window chamber) are translatable to skeletal muscle, we delivered loaded polymer films to the spinotrapezius muscles of mice of the same strain and age and assessed changes in remodeling after 7 days.

We hypothesized, based on window chamber results, that FTY720 treatment would increase arteriolar vascular growth and SMA coverage of microvessels of the spinotrapezius muscle. Preliminary investigation revealed that implantation of polymer films between the fascia and the spinotrapezius muscle was successful, with minimal displacement in film location over time. Figure 7 shows representative intravital microscopy images 7 days postimplantation of FTY720-loaded PLAGA films in the spinotrapezius muscle (Fig. 7E) and the overlying subcutaneous tissue (Fig. 7A–D). Qualitative inspection revealed that FTY720 stimulated an arteriogenic response, classified by classic signs of arteriogenesis, including increased tortuosity and collateralization of branching microvascular networks in both the skin and the muscle (Fig. 7A, C, E). This increased tortuosity and collateralization was not observed in PLAGA-stimulated tissue (Fig. 7B, D).

Figure 8 shows representative whole-mount spinotrapezius muscles harvested after 7 days and immunostained

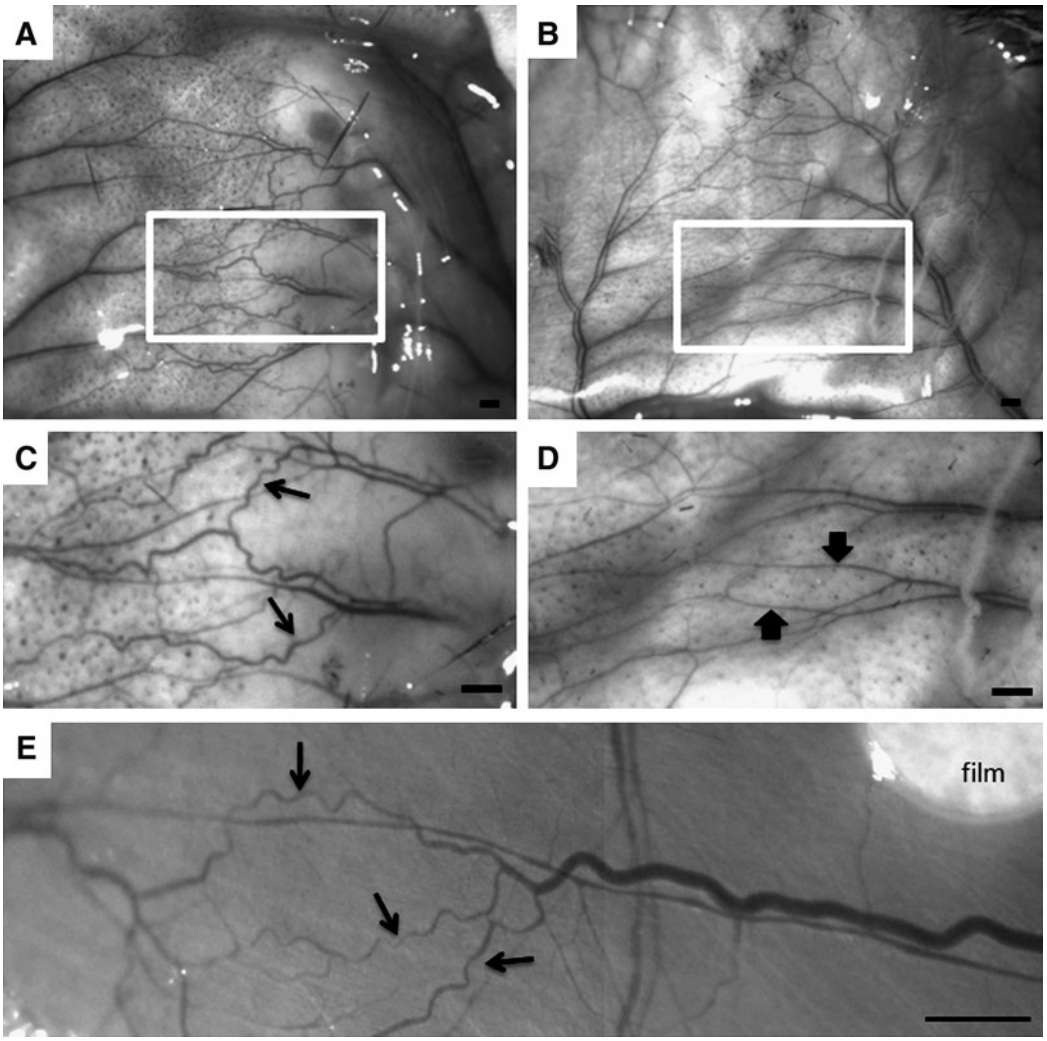

FIG. 7. Representative intravital microscopy images acquired during spinotrapezius surgeries at time of harvest on day 7. Images show the overlying subcutaneous tissue **(A–D)** and muscle tissue **(E)** after 7 days of treatment with FTY720 **(A, C)** compared to control PLAGA **(B, D)**. Classic signs of arteriogenesis, including collateralization and a tortuous vasculature **(C, E,** arrows**)**, are seen in FTY720-treated tissue, compared to control **(D,** arrows**)**. Outlined regions in **(A)** and **(B)** are shown magnified in **(C)** and **(D)**, respectively. Scale bars = 500 μm.

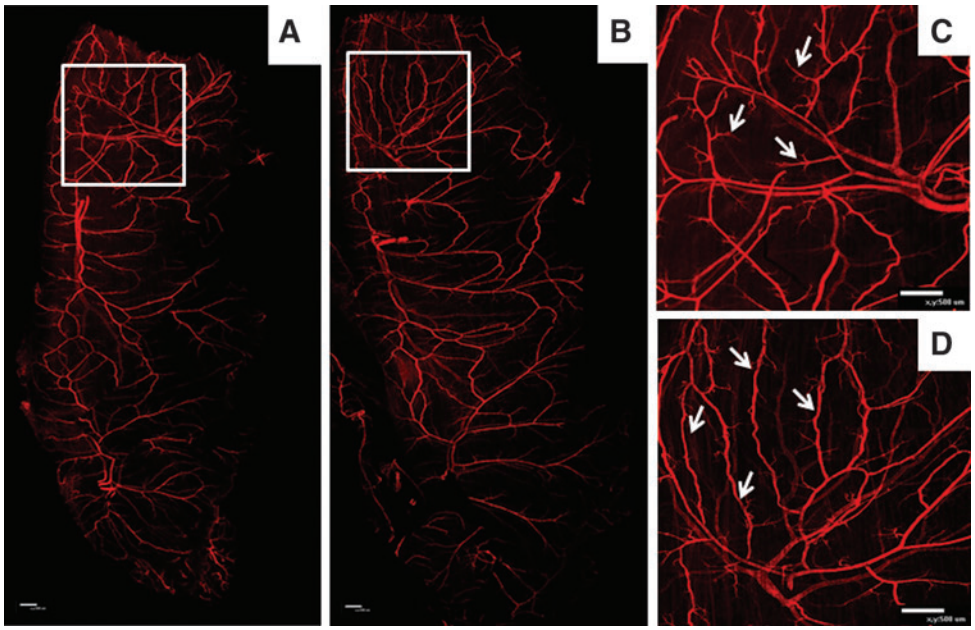

FIG. 8. FTY720 stimulates arteriogenesis in the mouse spinotrapezius muscle (whole-mount muscle tissue shown in **A, B**). Tissue was harvested after 7 days of treatment with FTY720 **(B, D)** or PLAGA **(A, C)** and stained with SMA. The approximate area of tissue affected by film implantation is denoted by white box **(A, B)**, with magnified images shown in **(C, D)**. Classic signs of arteriogenesis are seen in image **(D)** after treatment with FTY720, including collateral formation (arrows). Collaterals were not seen after treatment with PLAGA control polymer, as shown in **(C)** with arrows marking vascular branches. Scale bars 500 μm. Color images available online at www.liebertonline.com/ten.

with SMA. The left muscle served as a contralateral control and received no implant (not shown). FTY720-stimulated arteriogenesis in the mouse spinotrapezius muscle (Fig. 8B, D) compared to PLAGA control (Fig. 8A, C). The approximate area of tissue affected by film implantation is outlined by the white box in Figure 8A and B, with magnified images shown in Figure 8C and D. Classic signs of arteriogenesis[19] are seen in Figure 8D after treatment with FTY720, including collateral formation. Collaterals were not seen after treatment with PLAGA control polymer.

Discussion

We have previously reported that local, controlled release of S1P from biodegradable PLAGA constructs significantly enhanced the expansion of both arterioles and venules after 3 days of treatment in a murine dorsal skinfold window chamber model. This model is a useful tool for evaluating changes in microvascular remodeling because it allows for repeated measures and assessment of the same blood vessels over time to quantify growth and remodeling. The growth and structural enlargement of local microvessels was accompanied by a significant increase in BrdU-positive SMA-stained (SMA+) cells on the vessel wall, an observation suggestive of pharmacologically induced arteriogenesis.[15,23] Although local sustained release of S1P from PLAGA films allowed for therapeutically relevant concentrations of S1P to be made available to the microvasculature for extended growth, early arteriogenic remodeling was diminished by 7 days postimplantation and the effects of S1P stimulation were no longer statistically significant. In this study, we investigated whether the use of appropriately engineered agonists and antagonists of S1P receptors could be utilized to enhance the results of S1P-induced growth and maintenance of microvascular networks.

Vascular SMCs are able to rapidly undergo phenotypic modulation from a contractile quiescent state expressing SMC-specific differentiation genes (i.e., SMA, smooth muscle myosin heavy chain, SM22α) to a highly synthetic proliferative and migratory phenotype.[24] As a result of this unique characteristic, SMCs play a critical role in blood vessel development, remodeling, and maintenance and provide a therapeutic target for angiogenesis, atherosclerosis, and neointimal hyperplasia after vascular injury. In the latter case, our colleagues have demonstrated that acute balloon injury in the rat carotid artery leads to a significant increase in expression of $S1P_1$ and $S1P_3$ receptors and a significant decrease in $S1P_2$ receptor expression on SMCs up to 72 h postinjury. Additionally, pharmacological inhibition of $S1P_1$ and $S1P_3$ prevented S1P-induced SMC proliferation and potentiated expression of genes that define the contractile phenotype.[25] In the studies presented herein, pharmacological stimulation of $S1P_1$ and $S1P_3$ enhanced neovascularization and vessel maintenance, processes that require SMC proliferation, suggesting a potential phenotypic switch to the synthetic phenotype. Thus, manipulating the phenotypic modulation of vascular SMCs pharmacologically by strategically targeting known S1P receptor expression patterns could provide new avenues for growth of microvascular networks.

The major focus of these studies was to determine if we could pharmacologically manipulate the S1P signaling axis to promote microvascular growth and maturation *in vivo*. We used a library of S1P agonists and antagonists, namely, FTY720 ($S1P_1$, $S1P_3$, $S1P_4$, $S1P_5$ agonist), VPC01091 ($S1P_1$, $S1P_4$, $S1P_5$ agonist, $S1P_3$ antagonist), JTE013 ($S1P_2$ antagonist), and VPC44116 ($S1P_1$, $S1P_3$ antagonist). Codelivery of S1P with JTE013 acted as a pharmacological agonist at $S1P_1$, $S1P_3$, $S1P_4$, $S1P_5$ and antagonist at $S1P_2$, very similar to the actions of FTY720 but removing any potential contribution of $S1P_2$ signaling. S1P delivered with VPC44116 functioned as an $S1P_2$, $S1P_4$, $S1P_5$ agonist and $S1P_1$, $S1P_3$ antagonist and served to elucidate the synergistic importance of $S1P_1$ and $S1P_3$.

Results from the dorsal skinfold window chamber model show that stimulation of both $S1P_1$ and $S1P_3$ via delivery of agonist FTY720 enhances neovascularization and vessel maintenance; specifically, significant increases in lumenal

diameter expansion, vascular length density, and SMA+ vessels were observed in FTY720-treated tissues, compared to S1P and control samples. Additionally, FTY720 stimulation significantly increased the number of branch points on venules compared to PLAGA alone. FTY720 is a prodrug requiring phosphorylation by sphingosine kinase into FTY720-P, which is a potent agonist of $S1P_1$ and $S1P_3$ on vascular ECs and SMCs. Signaling of FTY720-P through the $S1P_1$ receptor has been shown *in vitro* to elicit similar cellular functions as S1P, including cell migration and proliferation, among others.[26] Our results *in vivo* support FTY720-induced increases in cell migration and proliferation, as evidenced by increased length density, diameter, and branching on venules, a metric indicative of sprouting angiogenesis.[3,27] In contrast, other studies have reported that FTY720 actually inhibits vascular endothelial growth factor-induced vascular permeability and angiogenesis.[28–30] The antiangiogenic effects of FTY720, though surprising based on its potent agonist activity, are proposed to occur as a result of functional antagonism. Although both S1P and FTY720 have been shown to internalize the $S1P_1$ receptor into the endosomal pathway, FTY720 induces ubiquitinylation and proteosomal degradation of the receptor.[31,32] Therefore, the $S1P_1$ receptor, after being bound by FTY720-P, is internalized and degraded, rendering it incapable of shuttling back to the cell surface for additional signaling. Interestingly, $S1P_3$ receptors remain functional throughout FTY720 treatment, suggesting that $S1P_3$ may be compensating for $S1P_1$ to elicit significant increases in length density and diameter expansion.[33]

The contribution of $S1P_3$ to vascular growth and maintenance was assessed using VPC01091. In contrast to FTY720 treatment, selective inhibition of $S1P_3$ by VPC01091 resulted in a significant reduction of length density and diameter expansion, as well decreased numbers of SMA+vessels. Taken together, the results of FTY720 and VPC01091 highlight the importance of $S1P_3$ in S1P-mediated microvascular remodeling and suggest that $S1P_1$ and $S1P_3$ must be acting synergistically to enhance SMC proliferation and/or migration to a level greater than what is achievable by activation of $S1P_1$ alone.

To retain spatial relationships and to study structurally defined whole-mounted networks in intact tissues, we also examined the effects of local FTY720 delivery in the spinotrapezius skeletal muscle of mice. The spinotrapezius is a pre-established model in an accessible tissue with a quick, minimally invasive surgery. Further, the spinotrapezius muscle is thin and flat, allowing whole network-level observation of the microvasculature *en face* using confocal microscopy.[18,19] FTY720 stimulated an arteriogenic response in the spinotrapezius muscle, classified by characteristic signs of arteriogenesis, including increased tortuosity and collateralization of branching microvascular networks in both the skin and the muscle.[4] This increased tortuosity and collateralization were not observed in PLAGA-stimulated tissue. Our results with local FTY720 delivery show some remarkable similarities in the network-level remodeling to spinotrapezius muscles receiving an arteriolar ligation.[18] Bailey *et al.* demonstrated arteriogenic remodeling in the spinotrapezius after ligation to a feeding arteriole in C57Bl/6 mice, marked by pronounced tortuosity, increased vascular density, increased branching, and collateral development.[18] Additional investigation using this model could lead to a more complete understanding of the role of $S1P_1/S1P_3$ synergism in microvascular remodeling, as well as new strategies to induce arteriolar remodeling on a larger, network-level scale.

JTE013 is a specific antagonist of $S1P_2$, activation of which has been shown to exert inhibitory effects on endothelial Rac activity, migration, and angiogenesis.[34] We hypothesized that by inhibiting $S1P_2$ receptor signaling with JTE013, while activating $S1P_1$ and $S1P_3$ signaling with coadministration of S1P, we could induce and maintain a synthetic phenotype in microvascular SMCs. In fact, sustained release of S1P+JTE013 significantly increased the diameter of arterioles and venules after 7 days compared to S1P treatment alone. Further, S1P+JTE013 treatment resulted in a significant expansion in venules relative to all comparative treatments, including FTY720. This discrepancy in arterial and venous responses to the same compound could be explained by differences in receptor expression patterns between the two vessel types,[35,36] but further validation is required. Unexpectedly, S1P+JTE013 delivery did not significantly increase functional length density; in fact, length density significantly decreased over the course of 7 days compared to FTY720 treatment, although not statistically different than treatment with S1P alone. Taken together, this suggests that the mechanism of action for S1P+JTE013-induced changes in length density likely varies from that of FTY720 treatment. Studies have linked the activation of $S1P_3$ by FTY720 to observations of enhanced neovascularization and blood flow recovery in ischemic hindlimbs through a mechanism involving CXCR4 activation and SDF-1-induced homing of circulating (CD34+) progenitor cells.[37] Recruitment of trafficking progenitor cells in response to FTY720 and their role in increasing microvascular growth and maintenance is currently being evaluated in our model.

Also notable, S1P+JTE013 responded similarly to S1P+VPC44116 ($S1P_1$, $S1P_3$ antagonist), which was hypothesized to significantly curtail FTY720-induced increases in length density due to its selective inhibition at $S1P_1$ and $S1P_3$. Our results with S1P+VPC44116 demonstrated a significant reduction in both venular diameter expansion and length density, compared to treatment with FTY720, suggesting a diminution in SMC proliferation. Interestingly, however, S1P+VPC44116 only moderately decreased arteriolar diameters in our model; we observed a 30% reduction in FTY720-increased arteriolar expansion compared to 140% reduction in venular expansion. These results suggest that although similar mechanisms of action are attenuating FTY720-induced diameter expansion, differences in receptor expression profiles on arterioles and venules may influence the magnitude of their respective responses. Also, $S1P_2$ is active in the presence of S1P+VPC44116. $S1P_2$-induced diminution of SMC proliferation is consistent with the published results of others, who showed that VPC44116 significantly reduced neointimal hyperplasia (SMC proliferation) after acute balloon injury of the rat carotid artery.[25] Selective activation of $S1P_2$ by S1P likely results in SMC phenotypic modulation to the contractile phenotype, with increased expression of SMA or other SMC differentiation marker genes.

The results of this study demonstrate that selective activation of $S1P_1$ and $S1P_3$ synergistically promotes S1P-induced increases in functional length density, arteriolar and venular diameter expansion, and proliferation of SMA+cells. Additionally, our group recently reported that local, controlled release of FTY720 significantly increased new bone formation,

total microvessel density, and SMC investment on new vessels in a cranial bone defect model.[38] The local release of FTY720 in a model of skeletal muscle also demonstrated robust arteriolar remodeling in SMA+vessels at the whole-network level, highlighting a potentially new role for FTY720 in areas where increased tissue perfusion are required. Collectively, these studies suggest that activation of $S1P_1$ and $S1P_3$ with FTY720 in the microvasculature may prove to be an effective strategy for promoting therapeutic angiogenesis and arteriogenesis in regions of ischemia or tissue insult.

Acknowledgments

Sources of support for this study include the National Institutes of Health grants K01AR052352-01A1, R01AR056445-01A2, R01DE019935-01, and R01GM067958 to Dr. Botchwey. Dr. Lauren Sefcik was supported by predoctoral fellowships from the National Science Foundation and American Heart Association Mid-Atlantic Affiliate 0815211E. Anthony Awojoodu is supported by the National Institutes of Health Biotechnology Training Program Training Grant T32GM008715.

Disclosure Statement

No competing financial interests exist.

References

1. Jain, R.K. Molecular regulation of vessel maturation. Nat Med **9,** 685, 2003.
2. Price, R.J., Owens, G.K., and Skalak, T.C. Immunohistochemical identification of arteriolar development using markers of smooth muscle differentiation. Evidence that capillary arterialization proceeds from terminal arterioles. Circ Res **75,** 520, 1994.
3. Benest, A.V., Stone, O.A., Miller, W.H., Glover, C.P., Uney, J.B., Baker, A.H., Harper, S.J., and Bates, D.O. Arteriolar genesis and angiogenesis induced by endothelial nitric oxide synthase overexpression results in a mature vasculature. Arterioscler Thromb Vasc Biol **28,** 1462, 2008.
4. Van Royen, N., Piek, J.J., Schaper, W., Bode, C., and Buschmann, I. Arteriogenesis: mechanisms and modulation of collateral artery development. J Nucl Cardiol **8,** 687, 2001.
5. Peirce, S.M., Price, R.J., and Skalak, T.C. Spatial and temporal control of angiogenesis and arterialization using focal applications of VEGF164 and Ang-1. Am J Physiol Heart Circ Physiol **286,** H918, 2004.
6. Kimura, T., Sato, K., Malchinkhuu, E., Tomura, H., Tamama, K., Kuwabara, A., Murakami, M., and Okajima, F. High-density lipoprotein stimulates endothelial cell migration and survival through sphingosine 1-phosphate and its receptors. Arterioscler Thromb Vasc Biol **23,** 1283, 2003.
7. Lee, H., Goetzl, E.J., and An, S. Lysophosphatidic acid and sphingosine 1-phosphate stimulate endothelial cell wound healing. Am J Physiol Cell Physiol **278,** C612, 2000.
8. Liu, Y., Wada, R., Yamashita, T., Mi, Y., Deng, C.X., Hobson, J.P., Rosenfeldt, H.M., Nava, V.E., Chae, S.S., Lee, M.J., Liu, C.H., Hla, T., Spiegel, S., and Proia, R.L. Edg-1, the G protein-coupled receptor for sphingosine-1-phosphate, is essential for vascular maturation. J Clin Invest **106,** 951, 2000.
9. Paik, J.H., Skoura, A., Chae, S.S., Cowan, A.E., Han, D.K., Proia, R.L., and Hla, T. Sphingosine 1-phosphate receptor regulation of N-cadherin mediates vascular stabilization. Genes Dev **18,** 2392, 2004.
10. Kluk, M.J., and Hla, T. Role of the sphingosine 1-phosphate receptor EDG-1 in vascular smooth muscle cell proliferation and migration. Circ Res **89,** 496, 2001.
11. Lockman, K., Hinson, J.S., Medlin, M.D., Morris, D., Taylor, J.M., and Mack, C.P. Sphingosine 1-phosphate stimulates smooth muscle cell differentiation and proliferation by activating separate serum response factor co-factors. J Biol Chem **279,** 42422, 2004.
12. Taha, T.A., Argraves, K.M., and Obeid, L.M. Sphingosine-1-phosphate receptors: receptor specificity versus functional redundancy. Biochim Biophys Acta **1682,** 48, 2004.
13. Goetzl, E.J., and Rosen, H. Regulation of immunity by lysosphingolipids and their G protein-coupled receptors. J Clin Invest **114,** 1531, 2004.
14. Rosen, H., and Liao, J. Sphingosine 1-phosphate pathway therapeutics: a lipid ligand-receptor paradigm. Curr Opin Chem Biol **7,** 461, 2003.
15. Sefcik, L.S., Petrie Aronin, C.E., Wieghaus, K.A., and Botchwey, E.A. Sustained release of sphingosine 1-phosphate for therapeutic arteriogenesis and bone tissue engineering. Biomaterials **29,** 2869, 2008.
16. Nickerson, M.M., Song, J., Shuptrine, C.W., Wieghaus, K.A., Botchwey, E.A., and Price, R.J. Influence of poly(D,L-lactic-co-glycolic acid) microsphere degradation on arteriolar remodeling in the mouse dorsal skinfold window chamber. J Biomed Mater Res A **91,** 317, 2009.
17. Murray, J. Angiogenesis protocols. Totowa, NJ: Humana Press, 2001.
18. Bailey, A.M., O'Neill, T.J., 4th, Morris, C.E., and Peirce, S.M. Arteriolar remodeling following ischemic injury extends from capillary to large arteriole in the microcirculation. Microcirculation **15,** 389, 2008.
19. Mac Gabhann, F., and Peirce, S.M. Collateral capillary arterialization following arteriolar ligation in murine skeletal muscle. Microcirculation **17,** 333, 2010.
20. Zhu, R., Snyder, A.H., Kharel, Y., Schaffter, L., Sun, Q., Kennedy, P.C., Lynch, K.R., and Macdonald, T.L. Asymmetric synthesis of conformationally constrained fingolimod analogues–discovery of an orally active sphingosine 1-phosphate receptor type-1 agonist and receptor type-3 antagonist. J Med Chem **50,** 6428, 2007.
21. Erdo, F., and Buschmann, I.R. Arteriogenesis: a new strategy of therapeutic intervention in chronic arterial disorders. Cellular mechanism and experimental models. Orv Hetil **148,** 633, 2007.
22. Lekas, M., Lekas, P., Latter, D.A., Kutryk, M.B., and Stewart, D.J. Growth factor-induced therapeutic neovascularization for ischaemic vascular disease: time for a re-evaluation? Curr Opin Cardiol **21,** 376, 2006.
23. Sefcik, L.S., Petrie Aronin, C.E., and Botchwey, E.A. Engineering vascularized tissues using natural and synthetic small molecules. Organogenesis **4,** 215, 2008.
24. Owens, G.K., Kumar, M.S., and Wamhoff, B.R. Molecular regulation of vascular smooth muscle cell differentiation in development and disease. Physiol Rev **84,** 767, 2004.
25. Wamhoff, B.R., Lynch, K.R., Macdonald, T.L., and Owens, G.K. Sphingosine-1-phosphate receptor subtypes differentially regulate smooth muscle cell phenotype. Arterioscler Thromb Vasc Biol **28,** 1454, 2008.
26. Sanchez, T., Estrada-Hernandez, T., Paik, J.H., Wu, M.T., Venkataraman, K., Brinkmann, V., Claffey, K., and Hla, T. Phosphorylation and action of the immunomodulator FTY720 inhibits vascular endothelial cell growth factor-induced vascular permeability. J Biol Chem **278,** 47281, 2003.

27. Thurston, G., Wang, Q., Baffert, F., Rudge, J., Papadopoulos, N., Jean-Guillaume, D., Wiegand, S., Yancopoulos, G.D., and McDonald, D.M. Angiopoietin 1 causes vessel enlargement, without angiogenic sprouting, during a critical developmental period. Development **132,** 3317, 2005.
28. Schmid, G., Guba, M., Ischenko, I., Papyan, A., Joka, M., Schrepfer, S., Bruns, C.J., Jauch, K.W., Heeschen, C., and Graeb, C. The immunosuppressant FTY720 inhibits tumor angiogenesis via the sphingosine 1-phosphate receptor 1. J Cell Biochem **101,** 259, 2007.
29. van Meeteren, L.A., Brinkmann, V., Saulnier-Blache, J.S., Lynch, K.R., and Moolenaar, W.H. Anticancer activity of FTY720: phosphorylated FTY720 inhibits autotaxin, a metastasis-enhancing and angiogenic lysophospholipase D. Cancer Lett **266,** 203, 2008.
30. LaMontagne, K., Littlewood-Evans, A., Schnell, C., O'Reilly, T., Wyder, L., Sanchez, T., Probst, B., Butler, J., Wood, A., Liau, G., Billy, E., Theuer, A., Hla, T., and Wood, J. Antagonism of sphingosine-1-phosphate receptors by FTY720 inhibits angiogenesis and tumor vascularization. Cancer Res **66,** 221, 2006.
31. Liu, C.H., Thangada, S., Lee, M.J., Van Brocklyn, J.R., Spiegel, S., and Hla, T. Ligand-induced trafficking of the sphingosine-1-phosphate receptor EDG-1. Mol Biol Cell **10,** 1179, 1999.
32. Oo, M.L., Thangada, S., Wu, M.T., Liu, C.H., Macdonald, T.L., Lynch, K.R., Lin, C.Y., and Hla, T. Immunosuppressive and anti-angiogenic sphingosine 1-phosphate receptor-1 agonists induce ubiquitinylation and proteasomal degradation of the receptor. J Biol Chem **282,** 9082, 2007.
33. Keul, P., Tolle, M., Lucke, S., von Wnuck Lipinski, K., Heusch, G., Schuchardt, M., van der Giet, M., and Levkau, B. The sphingosine-1-phosphate analogue FTY720 reduces atherosclerosis in apolipoprotein E-deficient mice. Arterioscler Thromb Vasc Biol **27,** 607, 2007.
34. Okamoto, H., Takuwa, N., Yokomizo, T., Sugimoto, N., Sakurada, S., Shigematsu, H., and Takuwa, Y. Inhibitory regulation of Rac activation, membrane ruffling, and cell migration by the G protein-coupled sphingosine-1-phosphate receptor EDG5 but not EDG1 or EDG3. Mol Cell Biol **20,** 9247, 2000.
35. Coussin, F., Scott, R.H., Wise, A., and Nixon, G.F. Comparison of sphingosine 1-phosphate-induced intracellular signaling pathways in vascular smooth muscles: differential role in vasoconstriction. Circ Res **91,** 151, 2002.
36. Mazurais, D., Robert, P., Gout, B., Berrebi-Bertrand, I., Laville, M.P., and Calmels, T. Cell type-specific localization of human cardiac S1P receptors. J Histochem Cytochem **50,** 661, 2002.
37. Walter, D.H., Rochwalsky, U., Reinhold, J., Seeger, F., Aicher, A., Urbich, C., Spyridopoulos, I., Chun, J., Brinkmann, V., Keul, P., Levkau, B., Zeiher, A.M., Dimmeler, S., and Haendeler, J. Sphingosine-1-phosphate stimulates the functional capacity of progenitor cells by activation of the CXCR4-dependent signaling pathway via the S1P3 receptor. Arterioscler Thromb Vasc Biol **27,** 275, 2007.
38. Petrie Aronin, C.E., Sefcik, L.S., Tholpady, S.S., Tholpady, A., Sadik, K.W., Macdonald, T.L., Peirce, S.M., Wamhoff, B.R., Lynch, K.R., Ogle, R.C., and Botchwey, E.A. FTY720 promotes local microvascular network formation and regeneration of cranial bone defects. Tissue Eng A **16,** 1801, 2010.
39. Saba, J.D., and Hla, T. Point-counterpoint of sphingosine 1-phosphate metabolism. Circ Res **94,** 724, 2004.
40. Butler, J., Lana, D., Round, O., and LaMontagne, K. Functional characterization of sphingosine 1-phosphate receptor agonist in human endothelial cells. Prostaglandins Other Lipid Mediators **73,** 29, 2004.
41. Osada, M., Yatomi, Y., Ohmori, T., Ikeda, H., and Ozaki, Y. Enhancement of sphingosine 1-phosphate-induced migration of vascular endothelial cells and smooth muscle cells by an EDG-5 antagonist. Biochem Biophys Res Commun **299,** 483, 2002.
42. Kawanabe, T., Kawakami, T., Yatomi, Y., Shimada, S., and Soma, Y. Sphingosine 1-phosphate accelerates wound healing in diabetic mice. Journal of dermatological science **48,** 53, 2007.
43. Inoki, I., Takuwa, N., Sugimoto, N., Yoshioka, K., Takata, S., Kaneko, S., and Takuwa, Y. Negative regulation of endothelial morphogenesis and angiogenesis by S1P2 receptor. Biochem Biophys Res Commun **346,** 293, 2006.

Address correspondence to:
Edward A. Botchwey, Ph.D.
Department of Biomedical Engineering
University of Virginia
PO Box 800759
Charlottesville, VA 22908

E-mail: botchwey@virginia.edu

Received: July 9, 2010
Accepted: September 27, 2010
Online Publication Date: November 2, 2010